Comparison of Multilayer Transparent Wood and Single Layer Transparent Wood With the Same Thickness

Yan Wu [1,2]*, Yajing Wang [1,2] and Feng Yang [3]*

[1]College of Furnishings and Industrial Design, Nanjing Forestry University, Nanjing, China, [2]Co-Innovation Center of Efficient Processing and Utilization of Forest Resources, Nanjing, China, [3]Fashion Accessory Art and Engineering College, Beijing Institute of Fashion Technology, Beijing, China

In this paper, poplar was used as raw material, sodium chlorite was used to delignify it in acidic environment, and then epoxy resin was vacuum impregnated in the delignified wood template to prepare transparent wood. Moreover, in order to imitate the lamination method of plywood, the multilayer transparent wood was prepared by means of staggered vertical lamination. The purpose of this paper is to study the physical and chemical properties of multilayer transparent wood, and to explore the application potential of multilayer transparent wood as a new material by comparing with single layer transparent wood with the same thickness. The weight of wood components in the transparent wood prepared in this experiment accounts for about 30–45% of the weight of composite materials. Scanning electron microscopy (SEM) measurements, Fourier transform attenuated total reflection infrared spectroscopy (ATR-FTIR) characterization, weight gain measurements, UV transmittance measurements, color difference measurements, water contact angle measurements and mechanical properties measurements were used to study. The results showed that as the thickness of the transparent wood increased, the cracks between the resin and the wood cell wall increased, and the interface showed an uneven state. In the case of the same thickness, the multilayer transparent wood was made by laminating transparent wood sheets, with fewer internal cracks and smooth interfaces. Its light transmittance is better than single layer transparent wood. Moreover, compared with single layer transparent wood with the same thickness, the lightness of multilayer transparent wood decreased, and tended to yellow and red. Due to the removal of lignin, the tensile strength of transparent wood decreased during the preparation process. However, it can be seen from the mechanical strength test that the tensile strength of multilayer transparent wood is much higher than that of single layer transparent wood. To a certain extent, multilayer transparent wood can improve the mechanical strength of transparent wood. To conclude, multilayer transparent wood is a kind of natural transparent material with large thickness, good light transmission and excellent mechanical properties, and it has a good development prospect.

Keywords: transparent wood, multilayer transparent wood, epoxy resin, acid delignification, thickness

INTRODUCTION

As a natural green material, wood has good physical and chemical properties, including high strength, low thermal conductivity, non-toxic, and biodegradable (Cabane et al., 2014; Vay et al., 2015). Therefore, wood is widely used in various fields, such as construction, furniture, and decoration (Iwamoto et al., 2005). In recent years, as people pay more attention to the global environment, more and more people have realized the importance of green and sustainable development (Xia et al., 2020), and wood, as the most abundant organic polymer resource on the earth, has also received more and more attention (Cabane et al., 2016; Wang et al., 2017). In addition, wood can be modified to improve some of its own defects, such as enhancing the hydrophilicity of wood surface, so as to better connect with adhesive (Wang et al., 2020). Moreover, the internal components of wood can also be extracted and applied, such as lignin applied to antioxidant components (Dong et al., 2020). In the past research, researchers also have developed modified wood with specific properties such as anti-corrosion wood, wood sponge, transparent wood, etc.

Transparent wood (TW) is a kind of wood with a certain light transmittance, which improves the opacity of the wood itself, and can be used as a new functional material to replace other light-transmitting materials, such as glass. Compared with glass, transparent wood has more excellent physical and chemical properties. The advantages of its wide range of raw materials, environmental protection in the manufacturing process, and excellent thermal stability can effectively solve the safety and environmental problems caused by the fragility of glass. Before the concept of transparent wood was proposed, transparent paper had been widely used in various fields. Transparent paper is prepared by extracting nano cellulose from wood and then modifying it. The method is to fill the holes in the paper with a substance with a refractive index similar to that of cellulose fibers and fillers to make the paper an optically uniform medium, in order to improve the transparency of paper (Gao et al., 2013; Jia et al., 2017). Similar to this method, in 1992, Fink (1992) first proposed the concept of transparent wood. It changed according to three different ways of light passing through a transparent object, namely, reflection, refraction and absorption on the outer surface and the inner surface. Therefore, the method of preparing transparent wood was proposed to first use a bleaching solution to chemically remove the lignin, and then fill the material with a refractive index similar to that of cellulose to eliminate the light scattering at the boundary between wood cells and obtain transparent wood. In 2016, Li et al. (2016) successfully prepared a transparent wood by impregnating the prepolymerized methyl methacrylate (PMMA) into the nanoporous cellulose template. This transparent wood has a light transmittance of 85% and a haze of about 70%. Moreover, by compressing the wood template, Li et al. changed the volume proportion of cellulose in transparent wood, thus adjusting the optical properties of transparent wood. This paper combines the function and structure of transparent wood, which lays a good foundation for further optimization of transparent wood technology. Zhu et al.

(2016) selected the radial cutting direction (R-wood) and longitudinal cutting direction (L-wood) of balsa wood as experimental materials to prepare transparent wood considering the structural characteristics of wood anisotropy. Comparing R-wood and L-wood of the same thickness, it was found that the transparency and haze of R-wood are higher than that of L-wood, while the mechanical strength of R-wood is lower than that of L-wood. It is proved that wood has different characteristics in different directions. Considering the practical use of transparent wood as a kind of structural timber, L-wood was used in this paper.

In addition to the research on the structure of transparent wood, the preparation method of transparent wood is also one of the topics that researchers focus on. According to the transparency principle of wood, the preparation of transparent wood can be divided into two parts, that is, decolorization and impregnating resin. The decolorization treatment is mainly to remove the light-absorbing substances in the wood, that is, lignin, and to provide channels for subsequent resin impregnation. At present, the commonly used decolorization treatment methods can be divided into two categories: removing lignin and modifying lignin. The main chemicals used to remove lignin are sodium hypochlorite, sodium chlorite and sodium sulfite. Sodium hypochlorite destroys the aromatic ring structure of lignin through oxidation and chlorination, so as to achieve the effect of removing lignin. For example, Jia et al. (2017) bleached balsa wood with 5% sodium hypochlorite solution to achieve the purpose of delignification. Sodium chlorite decomposes chlorine, chlorine dioxide and water by generating unstable chlorous acid in an acidic environment. These substances can degrade and dissolve lignin. This is currently one of the most widely used decolorization processes. Li et al. (2016), Tang et al. (2018), Gan et al. (2017), Vasileva et al. (2017) all used sodium chlorite solution to successfully prepare delignified wood templates under acidic conditions. Sodium sulfite is in an alkaline environment, through the reaction of SO^{3-} and lignin, the lignin is sulfonated and then dissolved in water, thereby achieving the function of delignification. This method Li et al. (2016) and Yu et al. (2017) are used in the preparation of transparent wood. Considering that the above methods can effectively remove lignin to achieve the effect of wood decolorization, but it will cause certain pollution to the environment. In 2017, Li et al. (2017) proposed a new environment-friendly method, which retained 80% of the lignin. By modifying the lignin, the chromogenic groups were removed, so as to achieve the purpose of decolorization. The impregnation resin part is mainly for the choice of resin. At present, the commonly used resins are polymethyl methacrylate (PMMA), epoxy resin and polyvinylpyrrolidone (PVP). Considering the process and cost comprehensively, this experiment uses sodium chlorite as a decolorizing agent to decolorize the wood, and then selects epoxy resin as the impregnating resin to fill the pores of the wood to prepare transparent wood.

As a structural material, transparent wood can be actually used in energy-saving buildings. In 2019, Li et al. (2019) used 2–5 cm thick translucent wood composite materials as the wall structure, and

demonstrated the huge potential of translucent wood as a new type of energy-saving building material by means of models. In 2020, Mi et al. (2020) prepared a beautiful and transparent wood with high light transmittance, high haze, and excellent UV resistance. It can be used as materials such as house walls and ceilings to effectively provide light to the room. However, the development of transparent wood is still restricted by thickness and material. At present, the thickness of transparent wood can only reach a few centimeters, and the raw materials used are mostly porous wood with lighter density, such as balsa wood, beech wood, etc., which are restricted by mechanical strength in the actual application process. Therefore, increasing the thickness of transparent wood is a topic that researchers are more concerned about. However, it is difficult to immerse the chemicals in the thick wood, so the expected experimental results cannot be achieved. Foster et al. (2019) thought that the current research on transparent wood mainly focuses on single layer transparent wood, and the excellent mechanical properties of multilayer transparent wood are also worthy of attention. They prepared 1-layer and 2-layer transparent wood, and proved that the multilayer board has better mechanical properties through the comparison of mechanical properties. Chen et al. (2019) also pointed out that most of the previous studies focused on the total transmittance of transparent wood at a specific thickness and the angular distribution of light passing through transparent wood at different thickness. They proposed that the light scattering, haze and transmittance can be adjusted by surface modification or lamination of the delignified wood template, which laid a foundation for the preparation of multilayer transparent wood. In addition, Qin et al. (2018) studied the preparation and properties of multilayer transparent wood from different tree species. He used balsa wood, paulownia wood, and white basswood as raw materials to laminate transparent veneers in the same direction and cross-laminated. This method prepared transparent multilayer wood, compared the light transmittance and mechanical properties of the two lamination methods. It was concluded that the cross-laminated method could improve the anisotropy of wood and eliminate the difference between the parallel and cross grain tensile, which had great advantages.

This experiment imitates the production process of plywood, that is, odd layer laminated veneer, and each layer of fiber is perpendicular to each other (Liu et al., 2010) to prepare multilayer transparent wood. Poplar wood was used as raw material to prepare delignified wood template by using sodium chlorite, and then transparent wood was prepared by placing it in epoxy resin impregnation solution. The physical and chemical properties of multilayer transparent wood and single layer transparent wood with the same thickness were compared in order to prepare transparent wood with thicker thickness and better mechanical properties, so as to broaden the application range of transparent wood.

EXPERIMENTAL PART

Materials
Poplar log(OW) is provided by Shantou Yihua life science and Technology Co., Ltd. The specifications used are shown in **Table 1**. The air-dry density of poplar is 0.113 g/cm^3, the absolute dry density is 0.087 g/cm^3, and the moisture content is 10.543%. Among them, as shown in **Figure 1**, the fiber direction 0° refers to the fiber arrangement direction, and 90° refers to the direction perpendicular to the fiber.

Sodium chlorite, concentration 80%, provided by Shanghai Macklin Co., Ltd. Glacial acetic acid, analytical grade, provided by Nanjing Chemical Reagent Co., Ltd. Anhydrous ethanol, analytically pure, provided by Nanjing Chemical Reagent Co., Ltd. E51 type epoxy resin is a low-molecular liquid bisphenol A type epoxy resin, provided by Kunshan Jiulimei Electronic Materials Co., Ltd., its epoxy value (equivalent/100 g) = 0.48–0.54, viscosity (mpas/25°C) is 11000–14000, volatile matter (%) ≤ 2, color number ≤ 2. B210 type epoxy resin curing agent is a new type of amine greenhouse curing agent modified by polyetheramine. It is provided by Kunshan Jiulimei Electronic Materials Co., Ltd. Its viscosity (mpas/25°C) is 200–300, The relative density at 20°C is 1.03–1.08 g/cm^3, and the amine value (KOHmg/g) is 300–400.

Electric heating constant temperature blast drying oven, model: DHG-9643BS-III, provided by Shanghai Xinmiao Medical Equipment Manufacturing Co., Ltd. Electronic balance, model: UTP-313, provided by Shanghai Huachao Electric Co., Ltd. ScienceTOOL laboratory oil-free vacuum pump, Model: R410, provided by American Saints International Group. Plastic vacuum dryer, Model: PC-3, provided by Shanghai Sanmu Industrial Co., Ltd. Digital display three-purpose constant temperature water tank, model: HH-600, provided by Jintan Provided by City Guowang Experimental Instrument Factory. Heat-collecting constant temperature heating magnetic stirrer, model: DF-101Z, provided by Nanjing Wozhong Instrument Equipment Co., Ltd.

Experimental Methods
In this experiment, sodium chlorite was used to prepare delignified wood template under acidic conditions. Then, the material with a refractive index similar to that of cellulose was filled into the wood pores to obtain transparent wood. In addition, a single layer transparent wood sheet was laminated and composited into a multilayer transparent wood by a staggered vertical lamination method.

Pre-Processing
The poplar was dried in an electric heating constant temperature blast drying oven, at 102°C for 12 h.

Preparation of the Wood Templates
A sodium chlorite aqueous solution with a concentration of 3.5 wt% was prepared, a glass rod was used to stir evenly, then an appropriate amount of glacial acetic acid was dropped into the solution, the pH value of the solution was adjusted to 4.6, and the delignified solution was obtained after stirring evenly again. The absolutely dry poplar was put into the delignification solution. Then, a digital display and a three-purpose thermostat water tank was used to keep the solution temperature at 85°C. The poplar was taken out after 4–8 h of reaction. The extracted poplar wood was washed with distilled water for three times, and the delignification solution on the surface was removed, and then dehydrated in absolute ethanol for 24 h to obtain the delignified wood templates.

TABLE 1 | Raw material specifications of poplar.

Thickness (h)/mm	Length (L)/mm	Width (b)/mm	Fiber direction	Air-dry quality (M_1)/g	Absolute dry quality (M_0)/g
0.5	40	20	0°/90°	0.067	0.062
1.5	40	20	0°	0.116	0.105
2.5	40	20	0°	0.151	0.137
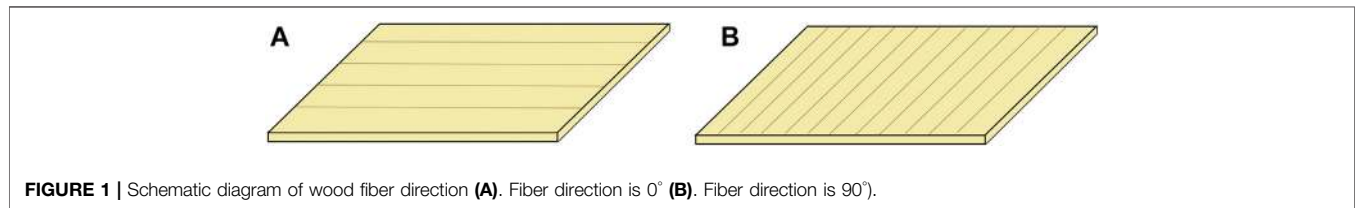
FIGURE 1 | Schematic diagram of wood fiber direction **(A)**. Fiber direction is 0° **(B)**. Fiber direction is 90°).
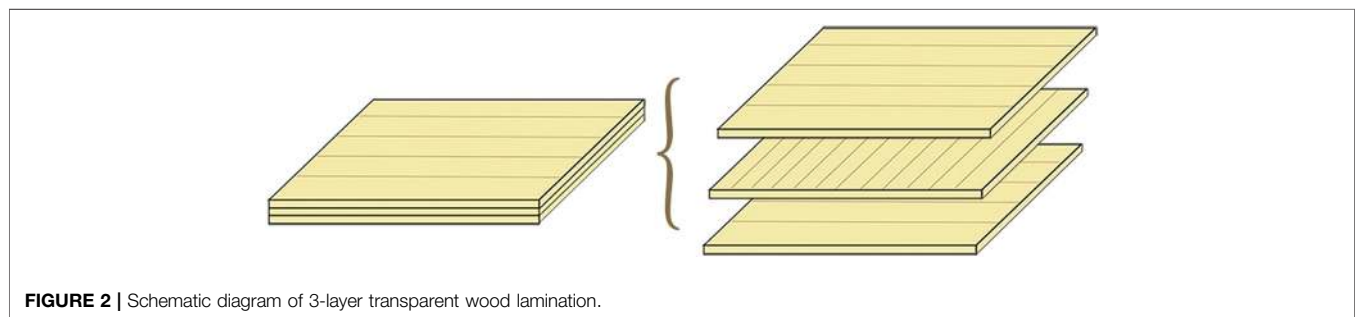
FIGURE 2 | Schematic diagram of 3-layer transparent wood lamination.

Preparation of the Transparent Wood

The delignified wood template was put into a plastic vacuum dryer. Then, an oil-free vacuum was used to pump it into vacuum, and dry it in vacuum for 10–20 min. The epoxy resin impregnation solution was prepared according to the weight ratio of epoxy resin to curing agent of 2:1, which was stirred evenly with a magnetic stirrer for standby. After vacuum drying, the appropriate amount of epoxy resin impregnation solution was poured into the delignified wood template, and it was immersed in vacuum environment for 25–30 min. Finally, the impregnated samples were taken out and placed in two pieces of silica gel to cure at room temperature in a vacuum environment for 12 h to obtain the transparent wood.

Preparation of the Multilayer Transparent Wood

The samples which were vacuum impregnated with epoxy resin impregnation solution for 25–30 min were taken out, and then they were laminated. As shown in **Figure 2**, **3**, 3-layers of transparent wood (0°/ 90°/ 0°) and 5-layers of transparent wood (0°/ 90°/ 0°/ 90°/ 0°). Then put them in two pieces of silica gel, clamp them with a clamp, give them a certain pressure, cure at room temperature in a vacuum environment for 12 h to obtain multilayer transparent wood.

Characterization

In order to facilitate the description of the characterization of the samples, this study numbered the sample types that would appear in the test. Specifically, A refers to poplar logs with a thickness of 0.5 mm and a fiber direction of 0°. DW-A refers to a delignified wood template with a thickness of 0.5 mm and a fiber direction of 0°. TW-A refers to transparent wood with a thickness of 0.5 mm and a fiber direction of 0°. B refers to poplar logs with a thickness of 0.5 mm and a fiber direction of 90°. DW-B refers to a delignified wood template with a thickness of 0.5 mm and a fiber direction of 90°. TW-B refers to transparent wood with a thickness of 0.5 mm and a fiber direction of 90°. C refers to a 1.5 mm thick poplar log with a fiber direction of 0°. DW-C refers to a delignified wood template with a thickness of 1.5 mm and a fiber direction of 0°. TW-C refers to transparent wood with a thickness of 1.5 mm and a fiber direction of 0°. D refers to poplar logs 2.5 mm thick and with a fiber direction of 0°. DW-D refers to a delignified wood template with a thickness of 2.5 mm and a fiber direction of 0°. TW-D refers to 2.5 mm thick transparent wood with a fiber direction of 0°. OW-3 refers to three layers of poplar logs. DW-3 refers to the 3-layer delignified wood template. TW-3 refers to three layers of transparent wood. OW5 refers to five layers of poplar logs. DW-5 refers to 5-layer delignified wood template. TW-5 refers to five layers of transparent wood.

Scanning Electron Microscope Measurements

The sample was cut along the transverse direction, and the surface of the cut sample was polished by ultra-thin slicer, and then adhered to the observation disk for vacuum gold plating. Then, the gold-plated samples were put into a scanning electron
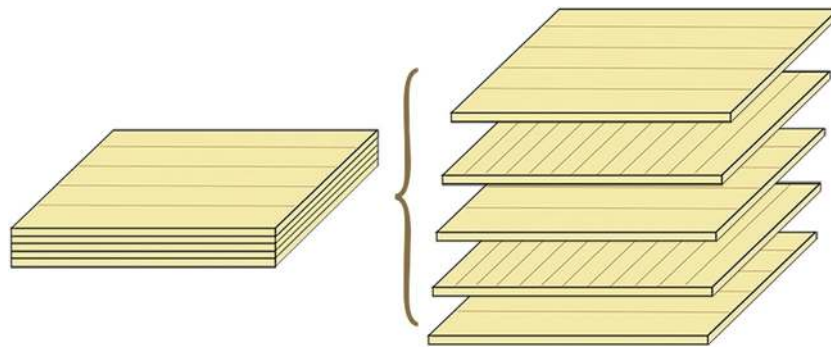
FIGURE 3 | Schematic diagram of 5-layer transparent wood lamination.

microscope (model: Quanta 200, provided by Fei Co., Ltd.) to observe the changes of pores and interfaces before and after treatment.

Fourier Transform Attenuated Total Reflection Infrared Spectroscopy Characterization

A Fourier Transform Infrared Spectrometer (Model VERTEX 80V, provided by Bruker Spectrometer Company, United States) was used to test and analyze the chemical groups in the sample. By observing the chemical group vibration of the sample under light irradiation with a wavenumber of 400–$4,000 \, cm^{-1}$, the changes in the chemical group of the sample before and after processing were analyzed.

Weight Gain Rate Measurements

The samples before and after impregnation were placed on an electronic balance (model: UTP-313, provided by Shanghai Huachao Electric Co., Ltd.) for measurement, and the weight gain rate was calculated according to **Eq. 1**. The weight gain rate of different thickness samples was compared, and the difference of weight gain rate between multilayer transparent wood samples and transparent wood with the same thickness was compared.

$$W = \frac{M_a - M_b}{M_b} \times 100\% \tag{1}$$

In formula, W represents weight gain rate, M_a represents mass after impregnation, M_b represents mass before impregnation.

UV Transmittance Measurements

TW samples with different thickness and multilayer transparent wood were tested by ultraviolet visible light photometer (model: Lambda 950, provided by PerkinElmer company, United States), and the transmittance of transparent wood samples was obtained in the visible light range, that is, the wavelength of 350–$800 \, nm$. The difference of light transmittance between multilayer transparent wood and transparent wood with the same thickness was compared. At the same time, in order to improve the accuracy of the data, samples under the same experimental conditions were selected for more than two repeated tests.

Color Difference Measurements

Color analysis of each sample was performed by PANTON color detector (model: RM200, provided by Ashley Co., Ltd.). Record the $L*a*b$ value of each sample, and analyze the color difference of samples before and after treatment. In order to reduce the test error, this test selects three points on the same sample to record respectively, and then calculates the average value to get the relatively accurate $L*a*b$ value. In order to ensure the same background color during the test, the samples were placed on A4 paper for testing.

Water Contact Angle Measurements

The contact angle tester [model: drop shape analyzer (DSA) 100 s, provided by Kruss Scientific Instruments Shanghai Co., Ltd.] was used to measure the surface properties of the samples before and after treatment. The contact angle of water droplets on the surface of the samples was observed, and the hydrophobicity of the samples before and after treatment was compared.

Mechanical Performance Measurements

The longitudinal tensile test was carried out on the original sample, delignified sample and transparent sample by the precise electronic mechanics experimental machine (model: AG-IC, provided by Shimadzu production Institute, Japan). The tensile rate was set at $5 \, mm/min$ and the maximum load force was $10,000 \, N$. Recorded the maximum tensile load, compared the change of tensile strength before and after treatment, and compared the tensile strength of multilayer transparent samples and transparent samples with the same thickness.

RESULTS AND DISCUSSION

Scanning Electron Microscope Analysis

The changes of porosity of wood before and after treatment were observed by SEM. As shown in **Figure 4**, the cross-sectional pores of sample A and B have changed after delignification and transparency treatment. Both sample A and B are poplar
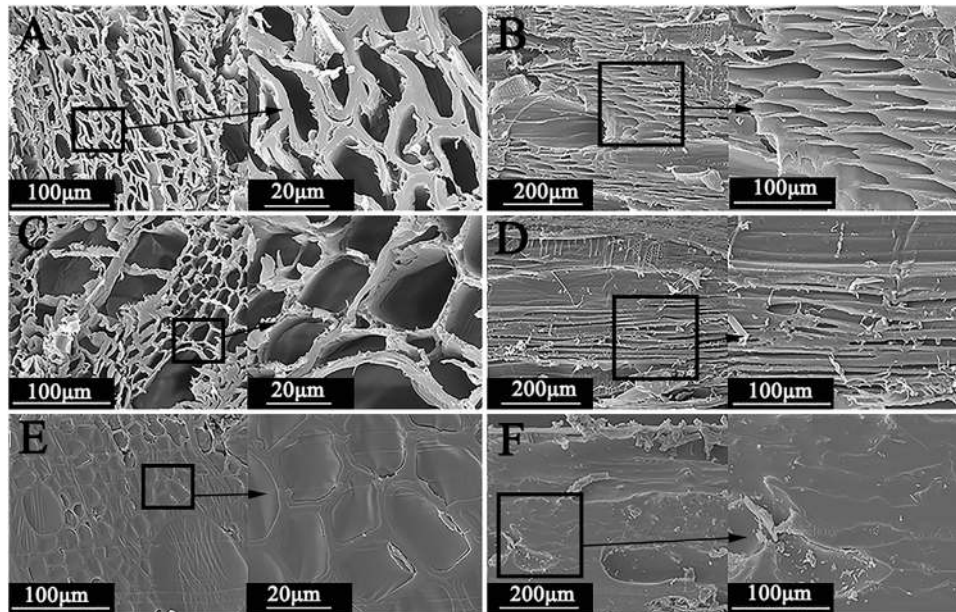
FIGURE 4 | SEM image of poplar with thickness of 0.5 mm before and after treatment (**A**.A; **B**.B; **C**. DW-A; **D**. DW-B; **E**.TW-A; **F**.TW-B).

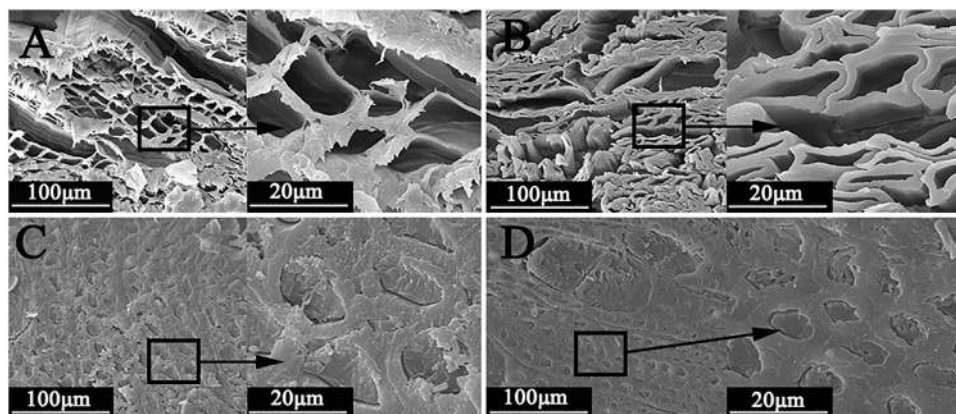FIGURE 5 | SEM image of poplar with thickness of 1.5 mm and 2.5 mm after delignification and transparency treatment (**A**. DW-C; **B**. DW-D; **C**.TW-C; **D**. TW-C).

wood with a thickness of 0.5 mm, but the fiber direction is different. **Figures 4A,B** show the internal pore structure of sample A and B before treatment. The parenchyma cells and tube pores of poplar can be seen from sample A, and the sectional morphology of parenchyma cells and tube pores can be seen in sample B. It can be seen from **Figure 4C** that after delignification, the cell wall of poplar sample becomes thinner, but the microstructure of the sample is not obviously damaged, and the original cell structure is still maintained. It can be seen from **Figures 4E,F** that the transparent sample contained epoxy resin material, and the interface between the epoxy resin and the wood itself cell wall is good after immersion treatment for the sample with the thickness of 0.5 mm, which is basically no crack (Fang et al., 2017).

It can be seen from **Figure 5** that the changes of thicker samples after delignification treatment and transparency treatment are roughly the same. However, by looking at **Figure 5B**, it can be found that the cell wall of the sample with a thickness of 2.5 mm undergoes swelling and shrinkage after delignification treatment. This is because compared with thin wood, thick wood needed to be soaked in a delignification agent for a longer period of time to remove lignin, and more deionized water was required for operation when washing the residual delignification agent in the wood. This caused thick wood to absorb more water, and the cell wall swelled more obviously. It can be seen from **Figures 5C,D** that there are obvious gaps at the junction between the resin and the cell wall, and there are obvious transverse cracks at the interface. Therefore, compared with the
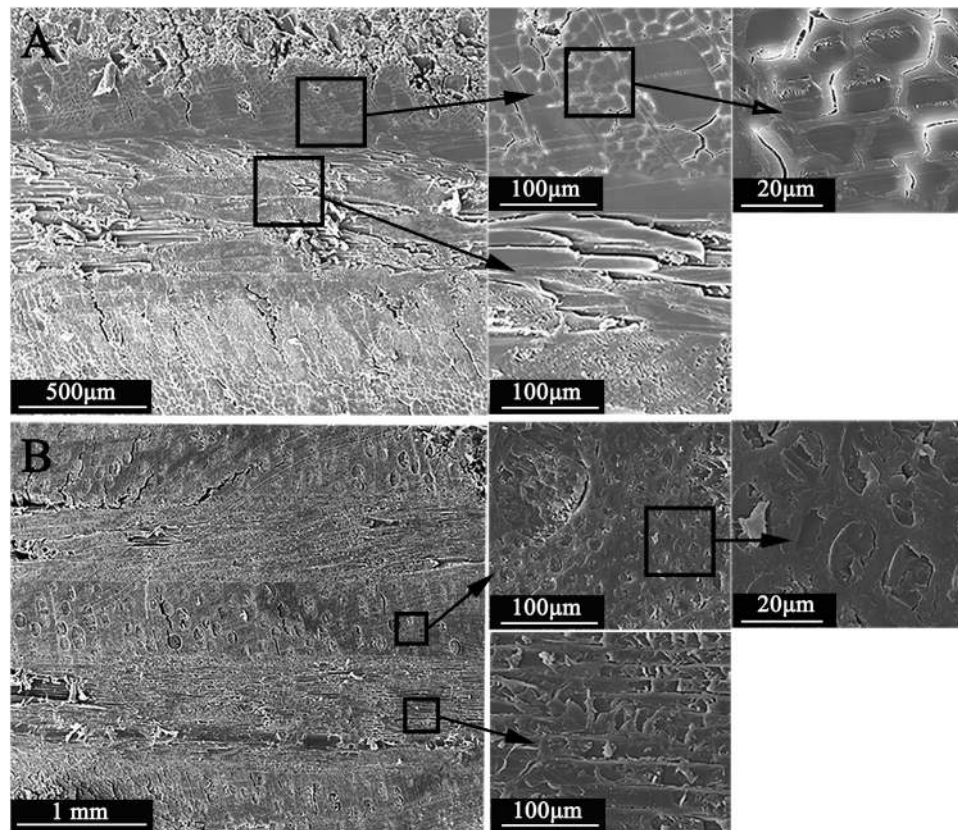
FIGURE 6 | SEM image of multilayer transparent wood (**A**.TW-3; **B**.TW-5).

thin transparent wood, the bonding degree of epoxy resin and wood cells in thick transparent wood is reduced.

It can be seen from **Figure 6** that the multilayer transparent wood was formed by staggered vertical lamination of thin wood, and obvious delamination interface can be seen at the splicing point. Compared with the transparent wood with the same thickness, the multilayer transparent wood has fewer internal cracks, and the epoxy resin has a better combination with the cell wall.

Fourier Transform Attenuated Total Reflection Infrared Spectroscopy Analysis
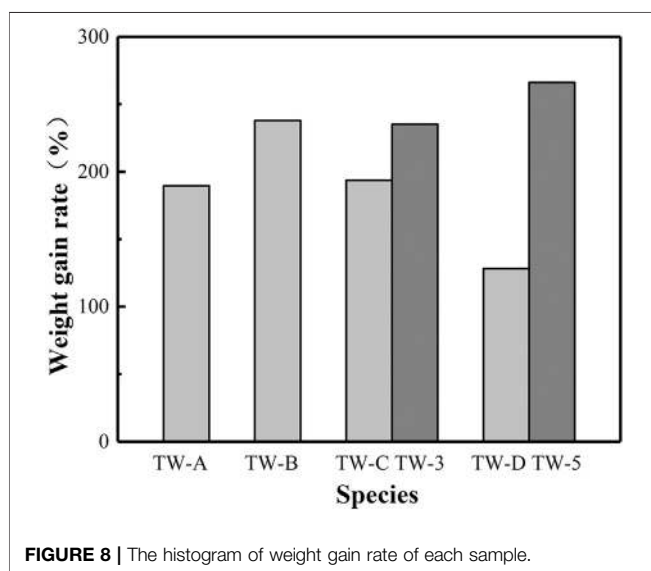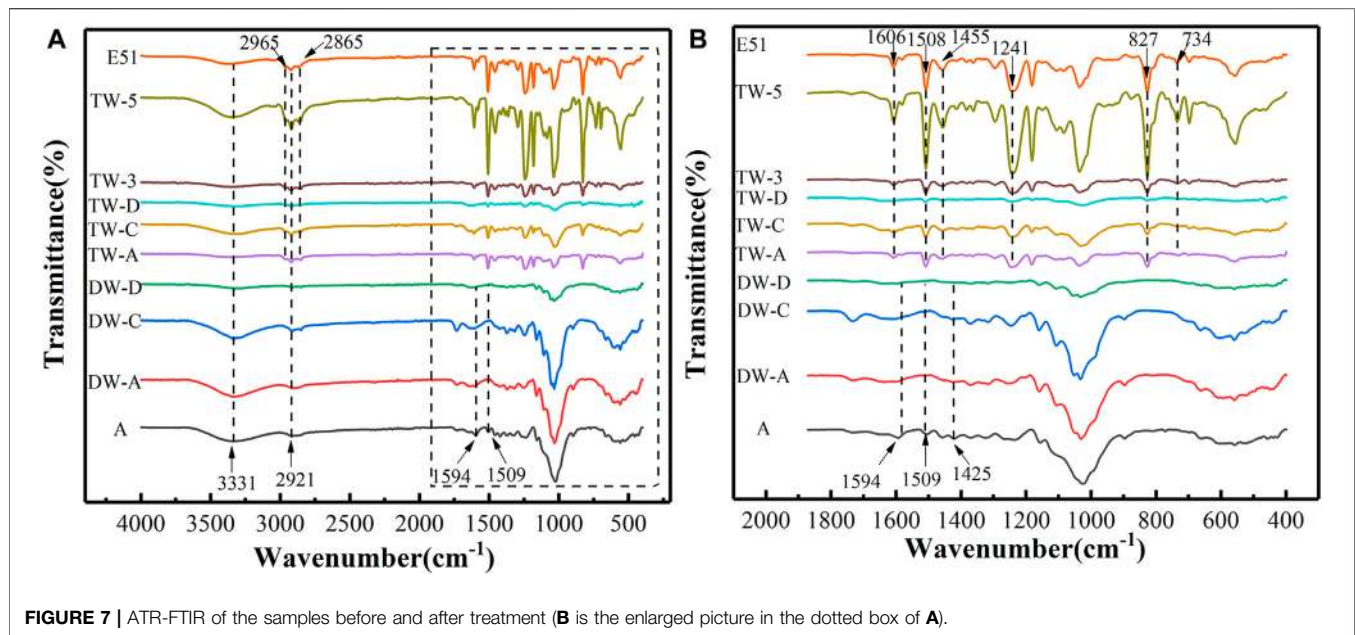
Since sample A and sample B are different only in fiber direction, sample A was selected for representative test. It can be seen from **Figure 7** that the absorption peaks of the original sample include the stretching vibration of O-H group at $3331 \, cm^{-1}$, the stretching vibration of C-H group at $2921 \, cm^{-1}$, the stretching vibration of $C = O$ group at $1594 \, cm^{-1}$, the stretching vibration of aromatic ring skeleton group of lignin at $1,509 \, cm^{-1}$ and the stretching vibration of $C = O$ group at $1,425 \, cm^{-1}$. The test results are consistent with the research results in the literature (Rana et al., 2010; Notburga et al., 2008). After delignification, the absorption peak at $1,509 \, cm^{-1}$ disappears in the infrared spectrum of delignified samples. This peak is the stretching vibration peak of

aromatic skeleton group of lignin, which prove that lignin was largely removed after delignification. The absorption peaks of E51 epoxy resin include the symmetric stretching vibration of the C-H group on CH_3 at a wavelength of $2,965 \, cm^{-1}$, the antisymmetric stretching vibration of the C-H group on CH_3 at 2,865, 1,606, and $1,508 \, cm^{-1}$. Besides, it include the asymmetric vibration band of the benzene ring skeleton at $1,455 \, cm^{-1}$, the scissor swing vibration of CH_3 at $734 \, cm^{-1}$, the stretching vibration of aliphatic ether C-O-C at $1,241 \, cm^{-1}$, the out of plane deformation of para substituted benzene ring of $= CH$ at $830 \, cm^{-1}$. It is consistent with the results of Zhao (2016). It can be seen from the figure that the infrared spectrum of the transparent sample obtained by vacuum impregnation of epoxy resin E51 has not only the characteristic absorption peak of delignified wood, but also the characteristic peak of epoxy resin E51.

Therefore, from the molecular point of view, the transparent sample contained the molecular groups in the delignified wood template and epoxy resin, and the epoxy resin was successfully polymerized with the delignified wood template.

Analysis of Weight Gain Rate

In the process of preparation, transparent wood needed to be impregnated with resin in vacuum, so that the refractive index of internal material was similar. According to **Eq. 1** in *Weight Gain Rate Measurements*, the weight gain rate of each sample

FIGURE 7 | ATR-FTIR of the samples before and after treatment (**B** is the enlarged picture in the dotted box of **A**).

FIGURE 8 | The histogram of weight gain rate of each sample.

imregnated with epoxy resin can be obtained, which reflects the different degree of epoxy resin impregnation in each sample. It can be seen from **Figure 8** that the weight gain rate of single layer transparent poplar wood with thickness of 0.5 and 1.5 mm is about 200%, but the transparent wood with thickness of 2.5 mm is restricted by the thickness direction, and the epoxy resin is difficult to be successfully impregnated into the interior of poplar, and the weight gain rate is greatly reduced, and the weight gain rate is only about 100%. Under the same initial thickness, the weight gain rate of multilayer transparent wood is greater than that of the single layer transparent wood with the same thickness. The weight gain rate of TW-3 is about 40% higher than that of TW-C, and that of TW-5 is about 140% higher

that of TW-D. The results show that the change of weight gain rate is obvious with the increased thickness.

At the same time, due to epoxy resin impregnation in poplar wood, the thickness of transparent sample wood also changed, as shown in **Table 2**, which is the thickness record table of OW and TW. Similar to the results of weight gain rate, the thickness change of multilayer transparent wood is more obvious than that of single layer transparent wood with the same thickness, and the change degree is more obvious with the increase of thickness.

UV Transmittance Analysis

It can be seen from **Figure 9** that OW are opaque under visible light. The light transmittance of TW-A is about 4%, that of TW-B is about 2%, and that of E51 epoxy resin is about 80%. The light transmittance increased with the increase of wavelength. When the visible light is 350–540 nm, the transmittance of TW-C is higher than that of TW-3; when the visible light is 540–800 nm, the transmittance of TW-C is lower than that of TW-3, and the longer the wavelength is, the greater the difference is. The transmittance curve of TW-D coincides with the OW curve, showing an opaque state, while TW-5 have a certain transmittance, and the longer the visible light wavelength is, the higher the transparency is.

It can be seen that the transmittance of transparent veneer with fiber direction of 0° is higher than that of transparent veneer with 90° fiber direction. For thicker samples, multilayer transparent wood can present a certain transmittance, while single layer transparent wood with the same thickness is restricted by the thickness direction, so it is difficult to deal with it, showing a basically opaque state. As shown in **Figure 10**, the macroscopic observation diagram is the same as the test result.

Color Difference Analysis

The $L*a*b$ color model consists of a lightness channel and two color channels. L represents the lightness, and the values are all

TABLE 2 | Thickness record of each sample before and after treatment.

Type	Thickness of OW (mm)	Thickness of TW (mm)
0.5 mm thick poplar wood with 0° fiber direction	0.50 (0.035)	0.68 (0.035)
0.5 mm thick poplar wood with 90° fiber direction	0.50 (0.035)	0.74 (0.025)
1.5 mm thick poplar wood	1.50 (0.026)	1.60 (0.090)
3-Layer poplar wood	1.50	—
*The relative thicknesses of different layers are all 0.5 mm	1.95 (0.068)	—
2.5 mm thick poplar wood	2.50	2.57 (0.040)
5-Layer poplar wood	2.50 (0.017)	—
*The relative thicknesses of different layers are all 0.5 mm	3.41 (0.225)	—

The values in brackets are the values of standard deviation.
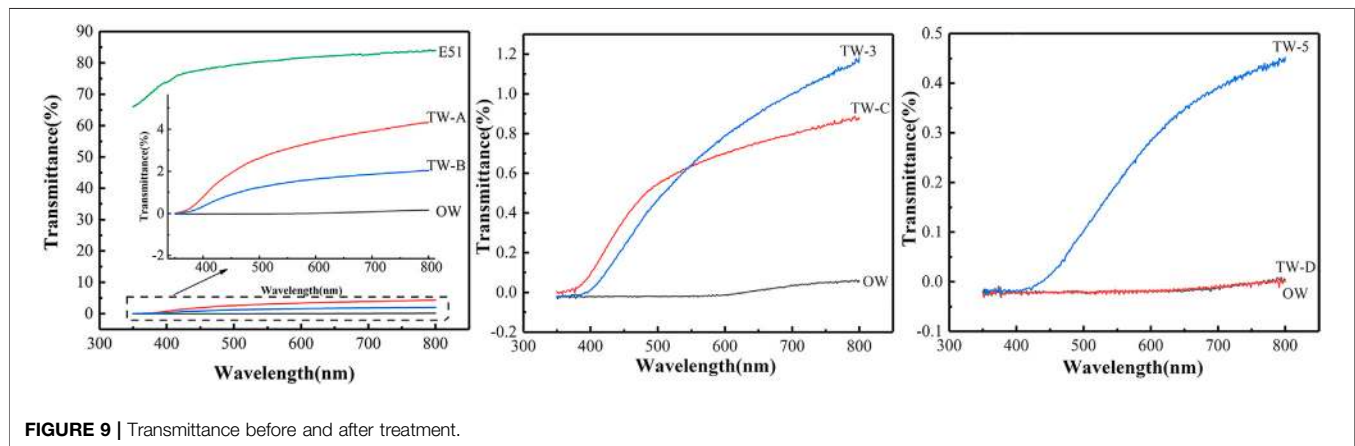
FIGURE 9 | Transmittance before and after treatment.
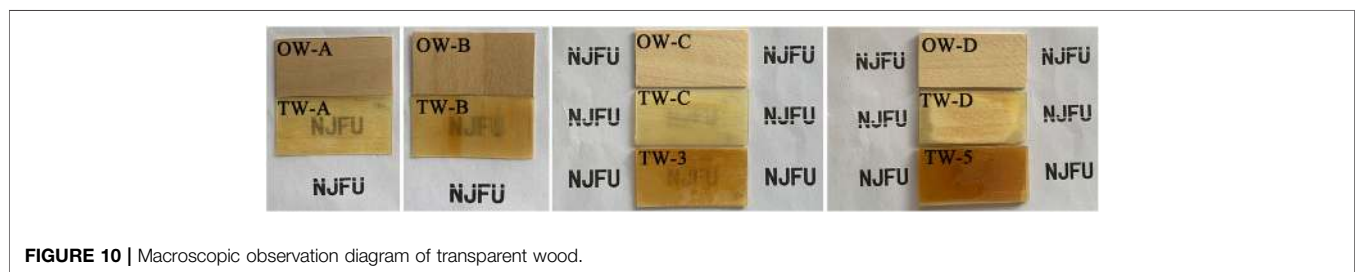
FIGURE 10 | Macroscopic observation diagram of transparent wood.

positive. The larger the value is, the higher the lightness is. a represents the range from green to red, and the value can be divided into positive and negative value. The larger the positive value is, the higher the red saturation of the object is, and the larger the negative value is, the higher the green saturation of the object is. b represents the range from blue to yellow, with positive and negative values. The larger the positive value is, the higher the yellow saturation of the object is, and the larger the negative value is, the higher the blue saturation of the object is (Jia et al., 2017). It can be seen from **Figure 11** that the L value of the single layer transparent sample increases after the transparent treatment, while the value of a and b have no obvious change, indicating that the brightness of the wood increases after the transparency treatment. Comparing multilayer transparent wood with single layer transparent wood with the same thickness, it can be found that the L value of TW-3 and TW-5 is lower than TW-C and TW-

D. a value of TW-3 and TW-5 is greater than TW-C. b value of TW-D, TW-3 and TW-5 is greater than that of TW-C and TW-D. This shows that with the same thickness, the brightness of the multilayer transparent wood is lower than that of the single layer transparent wood, and the color tends to be red and yellow. This is consistent with the macro picture shown in **Figure 10**. The multilayer transparent wood presents a transparent texture similar to amber.

Water Contact Angle Analysis

The test time was set to 100's, and the contact angle between the deionized water droplet and the sample surface was recorded every 5's to draw a broken line graph. It can be seen from **Figure 12** that poplar wood is a hydrophilic material, and deionized water droplets can be absorbed by poplar wood. When the transparent sample is about 20's, its contact angle
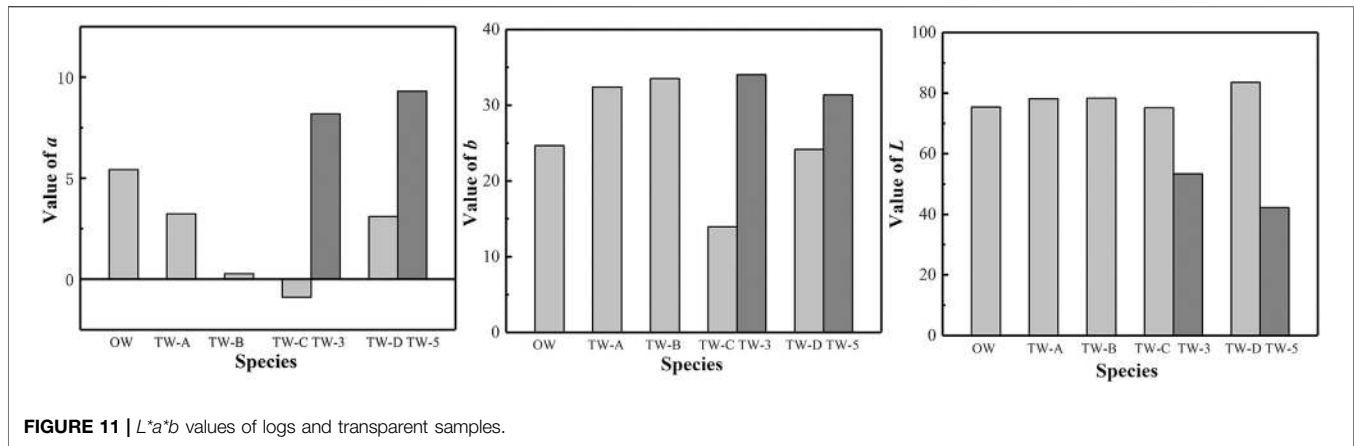
FIGURE 11 | L^*a^*b values of logs and transparent samples.
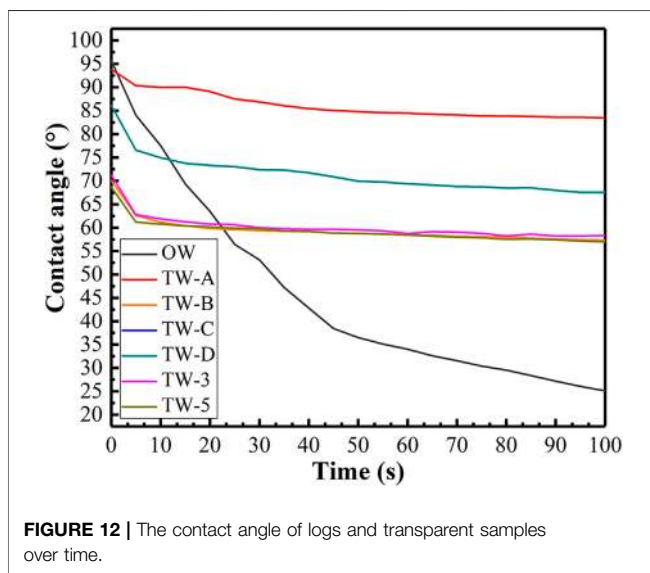

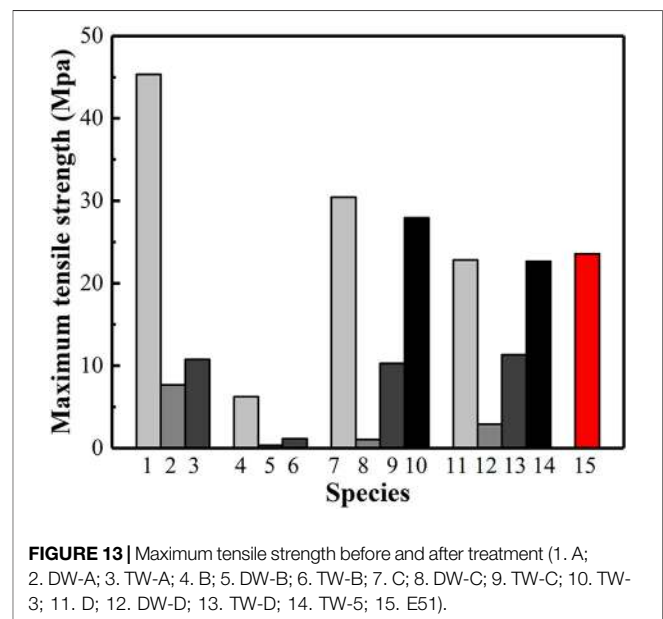**FIGURE 12 |** The contact angle of logs and transparent samples over time.

FIGURE 13 | Maximum tensile strength before and after treatment (1. A; 2. DW-A; 3. TW-A; 4. B; 5. DW-B; 6. TW-B; 7. C; 8. DW-C; 9. TW-C; 10. TW-3; 11. D; 12. DW-D; 13. TW-D; 14. TW-5; 15. E51).

begins to stabilize, showing a relatively stable state. This shows that transparent wood has improved the water absorption characteristics of wood to a certain extent, and can effectively reduce the wet expansion and shrinkage of wood due to moisture.

Mechanical Property Analysis

According to $p = F/S$, the maximum tensile strength of the sample can be calculated (Wu et al., 2020). In this text, S is the product of the h value and the b value in **Table 1**. From **Supplementary Material S1**, the weight loss of delignified wood and the weight proportion of wood components in transparent sample can be calculated. After delignification, the weight of wood will be reduced by 10–15%. It can be seen from **Figure 13** that after delignification, the maximum tensile strength of the sample is significantly reduced. However, after transparency treatment, the maximum tensile strength of the sample is improved, but it still does not reach the strength of the original sample. The weight of wood components in the single layer transparent wood prepared in this experiment accounts for 30–45% of the weight of composite materials, and the weight of

wood components in the multilayer transparent wood accounts for about 30% of the weight of composite materials. In addition, it could be found that the maximum tensile strength of single layer transparent wood was about 10°Mpa, while the maximum tensile strength of multilayer transparent wood could reach about 25°Mpa. Obviously, the maximum tensile strength of multilayer transparent wood is greatly improved compared with the transparent wood with the same thickness, which indicates that the tensile strength of multilayer transparent wood is better than that of single layer transparent wood with the same thickness.

CONCLUSION

Single layer transparent wood and multilayer transparent wood can be successfully prepared by the technology adopted in this study. The weight of wood components in the transparent wood prepared in this experiment accounts for about 30–45% of the

weight of composite materials. It can be seen from the SEM images that the greater the thickness of wood is, the more cracks on the interface between epoxy resin and wood cell wall are, showing unsmooth morphological characteristics. There are obvious delamination interfaces in the multilayer transparent wood, compared with the single layer transparent wood with the same thickness. The bonding cracks between epoxy resin and cell wall are less, and the morphology is relatively smooth.

The transparent wood has a certain light transmittance. With the increase of the thickness, the cracks between the cells and the resin inside the transparent wood become more obvious, which leads to the decrease of the transparency. While, compared with the single layer transparent wood with the same thickness, the resin in the multilayer transparent wood combines well with the cell wall, with smaller cracks and relatively flat interface. And through the UV transmittance test, we could find that the transmittance of multilayer transparent wood is greater than that of single layer wood with the same thickness. At the same time, compared with the original wood, the multilayer transparent wood has a certain color difference. Perhaps, this is related to the oxidation of hemicellulose, and the residue of sodium chlorite and lignin. Compared with the single layer transparent wood with the same thickness, the brightness of the multilayer transparent wood decreases, and tends to be yellow and red, showing a transparent texture similar to amber.

In the preparation process, due to the large amount of lignin released, the wood structure was damaged to a certain extent, and the tensile strength of the wood decreased. Compared with untreated wood, the tensile strength of transparent wood was weakened. Multilayer transparent wood can improve this weakness, and its tensile strength is greater than that of single layer transparent wood with the same thickness. In addition, transparent wood can improve the water absorption property of wood to a certain extent, and can effectively reduce the moisture swelling and drying shrinkage of wood due to moisture.

In conclusion, the transmittance and mechanical properties of multilayer transparent wood are better than that of single layer transparent wood. Compared with the single layer transparent wood with the same thickness, the resin in the multilayer transparent wood is better combined with the cell wall, so the light transmittance of the multilayer transparent wood is higher than that of the single-layer transparent wood of the same thickness, and as the thickness increases, this advantage becomes more obvious. Besides, the maximum tensile strength of multilayer transparent wood is more than two times that of single layer transparent wood with the same thickness. Combined with the current process conditions, transparent wood is restricted by the thickness direction. Therefore, multilayer

transparent wood can be prepared by lamination, so as to obtain materials with large thickness, high transmittance and excellent mechanical properties. Multilayer transparent wood has a good development prospect in the future.

DATA AVAILABILITY STATEMENT

The original contributions presented in the study are included in the article/**Supplementary Material**, further inquiries can be directed to the corresponding authors.

AUTHOR CONTRIBUTIONS

YWu contributed to conception and design of the study. YWa organized the database, performed the statistical analysis,and wrote the first draft of the manuscript. FY provided the funding support. All authors contributed to manuscript revision, read, and approved the submitted version.

FUNDING

ACKNOWLEDGMENTS

SUPPLEMENTARY MATERIAL

The Supplementary Material for this article can be found online at: https://www.frontiersin.org/articles/10.3389/fmats.2021.633345/full#supplementary-material.

REFERENCES

Cabane, E., Keplinger, T., Künniger, T., Merk, V., and Burgert, I. (2016). Functional lignocellulosic materials prepared by ATRP from a wood scaffold. *Sci. Rep.* 6, 31287. doi:10.1038/srep31287

Cabane, E., Keplinger, T., Merk, V., and Hass, P. (2014). Renewable and functional wood materials by grafting polymerization within cell walls. *ChemSusChem* 7, 1020–1025. doi:10.1002/cssc.201301107

Chen, H., Baitenov, A., Li, Y., Vasileva, E., Popov, S., Sychugov, I., et al. (2019). Thickness dependence of optical transmittance of transparent wood: Chemical modification effects. *ACS Appl. Mater. Interfaces* 11, 35451–35457. doi:10.1021/acsami.9b11816

Dong, H., Zheng, L., Yu, P., Jiang, Q., Wu, Y., Huang, C., et al.(2020). Characterization and application of lignin-carbohydrate complexes from lignocellulosic materials as antioxidants for scavenging *in vitro* and *in vivo* reactive oxygen species. *ACS Sustainable Chem. Eng.* 8, 256–266. doi:10.1021/acsuschemeng.9b05290

Fang, L., Xiong, X., Wang, X., Chen, H., and Mo, X. (2017). Effects of surface modification methods on mechanical and interfacial properties of high-density polyethylene-bonded wood veneer composites. *J. Wood Sci.* 63, 65–73. doi:10.1007/s10086-016-1589-9

Fink, S. (1992). Transparent wood - A new approach in the functional study of wood structure. *Holzforschung* 46, 403–408. doi:10.1515/hfsg.1992.46.5.403

Foster, K., Hess, K., Miyake, G., and Srubar, W.V. (2019). Optical properties and mechanical modeling of acetylated transparent qood composite laminates. *Materials* 12, 2256. doi:10.3390/ma12142256

Gan, W., Xiao, S., Gao, L., Gao, R., Li, J., and Zhan, X. (2017). Luminescent and transparent wood composites fabricated by poly(methyl methacrylate) and γ-Fe2O3@YVO4:Eu3+ nanoparticle impregnation. *ACS Sustainable Chem. Eng.* 5, 3855–3862. doi:10.1021/acssuschemeng.6b02985

Gao, K., Shao, Z., Wu, X., Wang, X., Li, J., Zhang, Y., et al. (2013). Cellulose nanofibers/reduced graphene oxide flexible transparent conductive paper. *Carbohydrate Polymers* 97, 243. doi:10.1016/j.carbpol.2013.03.067

Iwamoto, S., Nakagaito, A. N., Yano, H., and Nogi, M. (2005). Optically transparent composites reinforced with plant fiber-based nanofibers. *Appl. Phys. A.* 81, 1109–1112. doi:10.1007/s00339-005-3316-z

Jia, C., Li, T., Chen, C., Dai, J., Kierzewski, I. M., Song, J., et al. (2017). Scalable, anisotropic transparent paper directly from wood for light management in solar cells. *Nano Energy* 36, 366–373. doi:10.1016/j.nanoen.2017.04.059

Li, H., Guo, X., He, Y., and Zheng, R. (2019). House model with 2-5 cm thick translucent wood walls and its indoor light performance. *Eur. J. Wood Prod.* 77, 843–851. doi:10.1007/s00107-019-01431-w

Li, T., Zhu, M., Yang, Z., Song, J., Dai, J., Yao, Y., et al. (2016c). Wood composite as an energy efficient building material: guided sunlight transmittance and effective thermal insulation. *Adv. Energy Mater.* 6, 1601122. doi:10.1002/aenm.201601122

Li, Y., Fu, Q., Rojas, R., Yan, M., Lawoko, M., and Berglund, L. (2017). Lignin-retaining transparent wood. *ChemSusChem* 10, 3445–3451. doi:10.1002/cssc.201701089

Li, Y., Fu, Q., Yu, S., Yan, M., and Berglund, L. (2016a). Optically transparent wood from a nanoporous cellulosic template: Combining functional and structural performance. *Biomacromolecules* 17, 1358–1364. doi:10.1021/acs.biomac.6b00145

Li, Y., Yu, S., Veinot, J. G. C., Linnros, J., Berglund, L., and Sychugov, I. (2016b). Luminescent transparent wood. *Adv. Opt. Mater.* 5, 1600834. doi:10.1002/adom.201600834

Liu, X., Song, X., and Wu, Y. (2010). Study on hot-pressing technology of the chinese fir plywood. *Fujian Academy of Forestry* 37, 77–80. doi:10.3969/j.issn.1002-7351.2010.03.016

Mi, R., Chen, C., Keplinger, T., Pei, Y., He, S., Liu, D., et al. (2020). Scalable aesthetic transparent wood for energy efficient buildings. *Nat. Commun.* 11. doi:10.1038/s41467-020-17513-w

Notburga, G., Luna, G., Martin, S., Ingo, B., Catherine, C., Tilmann, R., et al. (2008). Situ FT-IR microscopic study on enzymatic treatment of poplar wood cross-sections. *Biomacromolecules* 9, 2194–2201. doi:10.1021/bm800300b

Qin, J., Bai, T., Shao, Y., Shao, X., Li, S., and Hu, Y. (2018). Preparation and characterization of multilayer transparent wood from different tree species. *J. Beijing For. Univ.* 40, 114–120.

Rana, R., Langenfeld-Heyser, R., Finkeldey, R., and Polle, A. (2010). FTIR spectroscopy, chemical and histochemical characterisation of wood and lignin of five tropical timber wood species of the family of Dipterocarpaceae. *Wood Sci. Technol.* 44, 225–242. doi:10.1007/s00226-009-0281-2

Tang, Q., Fang, L., Wang, Y., Zou, M., and Guo, W. (2018). Anisotropic flexible transparent films from remaining wood microstructures for screen protection and AgNW conductive substrate. *Nanoscale* 10, 4344–4353. doi:10.1039/c7nr08367j

Vasileva, E., Li, Y., Sychugov, I., Mensi, M., Berglund, L., and Popov, S. (2017). Lasing from organic dye molecules embedded in transparent wood. *Adv. Opt. Mater.* 5, 1700057. doi:10.1002/adom.201700057

Vay, O., De Borst, K., Hansmann, C., Ller, AT., and Muller, U. (2015). Thermal conductivity of wood at angles to the principal anatomical directions. *Wood Sci. Technol.* 49, 577–589. doi:10.1007/s00226-015-0716-x

Wang, Y., Sun, G., Dai, J., Chen, G., Morgenstern, J., Wang, Y., et al. (2017). A high-performance, low-tortuosity wood-carbon monolith reactor. *Adv. Mater.* 29, 1604257. doi:10.1002/adma.201604257

Wang, Z., Kang, H., Liu, H., Zhang, S., Xia, C., Wang, Z., et al. (2020). Dual-Network Nanocross-linking Strategy to Improve Bulk Mechanical and Water-Resistant Adhesion Properties of Biobased Wood Adhesives. *ACS Sustainable Chem. Eng.* 8, 16430–16440. doi:10.10.1021/acssuschemeng.0c04913

Wu, Y., Zhou, J., Huang, Q., Yang, F., Wang, Y., and Wang, J. (2020). Study on the properties of partially transparent wood under different delignification processes. *Polymers* 12, 661. doi:10.3390/polym12030661

Xia, C., Lam, S., and Sonne, C. (2020). Ban unsustainable mink production. *Science* 370, 1. doi:10.1126/science.abf0461

Yu, Z., Yao, Y., Yao, J., Zhang, L., Chen, Z., Gao, Y., et al. (2017). Transparent wood containing CsxWO3 nanoparticles for heat-shielding window applications. *J. Mater. Chem. A* 5, 6019–6024. doi:10.1039/C7TA00261K

Zhao, J. (2016). Study on the main performance characterization technology of bisphenol a epoxy resin system. Dissertation. Qingdao (China): Qingdao University of Science and Technology.

Zhu, M., Song, J., Li, T., Gong, A., Wang, Y., and Dai, J. (2016). Highly anisotropic, highly transparent wood composites. *Adv. Mater.* 28, 5181–5187. doi:10.1002/adma.201600427